Yu *et al. Geoscience Letters* (2024) 11:39
https://doi.org/10.1186/s40562-024-00352-8

Geoscience Letters

RESEARCH LETTER **Open Access**

Surface air temperature anomalies over Antarctica and the Southern ocean induced by interactions between the interdecadal Pacific oscillation and Atlantic multidecadal oscillation

Lejiang Yu[1], Shiyuan Zhong[2], Cuijuan Sui[3*] and Bo Sun[1]

Abstract

Previous research has explored the impact of the Interdecadal Pacific Oscillation (IPO) and Atlantic Multidecadal Oscillation (AMO) on Antarctic surface air temperature (SAT) variability. However, a notable gap remains in our comprehension concerning the response of Antarctic SAT to the four phase combinations of IPO and AMO. In this study, we unveil unique patterns of Antarctic SAT anomalies during four distinct sub-periods based on the phases of IPO and AMO. Notably, Antarctic SAT anomalies exhibit a considerable seasonality, with the most pronounced (weakest) anomalies occurring during the austral winter (summer), a phenomenon consistent across all four sub-periods. These different anomalous SST patterns trigger varying convective rainfall patterns, consequently initiating distinct wavetrains that propagate into the Southern Ocean. These different wavetrains, in turn, induce variations in sea level pressure and surface wind fields, resulting in different Antarctic SAT anomalies primarily through mechanisms related to horizontal thermal advection and downward longwave radiation.

Key points

- Antarctic SAT anomalies exhibit a considerable seasonality during the four combinations of the phases of the IPO and AMO.
- These different SST anomalies during the combinations trigger distinct wavetrains that propagate into the Southern Ocean.
- Different wavetrains induce anomalous sea level pressure and surface wind fields and Antarctic SAT through thermal advection and radiation.

Plain language summary

Understanding the variability in Antarctic surface air temperature (SAT) is crucial for unraveling the complex dynamics of the polar climate system and its broader implications for global climate patterns. Fewer studies highlighted the impacts of the four combinations of the phases of IPO and AMO on Antarctic SAT anomalies. In this study,

*Correspondence:
Cuijuan Sui
suicj@nmefc.cn
Full list of author information is available at the end of the article

we uncover distinct patterns of Antarctic SAT anomalies during four different periods based on the phases of IPO and AMO. We note that Antarctic SAT anomalies exhibit a considerable seasonality, with the most pronounced (weakest) anomalies occurring during the austral winter (summer), consistently across all four periods. The anomalous SST patterns during different periods trigger distinct wavetrains that propagate into the Southern Ocean, inducing variations in sea level pressure, surface wind fields, and Antarctic SAT anomalies. These findings bear substantial implications for the prediction of Antarctic seasonal SAT variations on interdecadal timescales.

Introduction

The Pacific decadal oscillation (PDO)/Interdecadal Pacific Oscillation (IPO) and the Atlantic Multidecadal Oscillation (AMO) are prominent drivers of sea surface temperature (SST) variability on interdecadal timescales (Mantua et al. 1997; Mantua and Hare 2002; Enfield et al. 2001; Henley et al. 2015; Newman et al. 2016). These well-documented climate phenomena are acknowledged for their interactions over decadal periods (d'Orgeville and Peltier 2007; Wu et al. 2011; Meehl et al. 2021; Hong et al. 2022). Such interactions are characterized by the PDO/IPO's ability to induce corresponding phases of the AMO (Cai et al. 2019; Meehl et al. 2021), and reciprocally, the AMO's capability to produce opposing phases of the PDO/IPO through the influence of Walker circulation anomalies and mid-latitude teleconnections (McGregor et al. 2014; Li et al. 2016a, b; Levine et al. 2017; Ruprich-Robert et al. 2017; An et al. 2021; Meehl et al. 2021).

The PDO/IPO plays a pivotal role in regulating surface air temperature (SAT) and precipitation patterns across the Asian monsoon region (Krishnan and Sugi 2003; Hessl et al. 2004; Chan and Zhou 2005; Wang et al. 2008; Chen et al. 2013; Krishnamurthy and Krishnamurthy 2014) and South America (Andreoli and Kayano 2005; Kayano and Andreoli, 2007). Additionally, it exerts a profound impact on polar SAT and sea ice cover (Meehl et al. 2013; 2016; 2018; 2019; Turner et al. 2016, 2020) and assumes a significant role in the interdecadal variability of global SAT and precipitation (Meehl et al. 2013; Kosaka and Xie 2013; Dong and Dai 2015). Conversely, the AMO has been associated with climatic and weather patterns in Europe (Sutton and Hodson 2005; Knight et al. 2006; Peings and Magnusdottir 2014; 2016), Atlantic hurricane activity (Vimont and Kossin 2007; Wang et al. 2012), the West African monsoon (Martin and Thorncroft 2014), and rainfall patterns in the Sahel region of Africa (Wang et al. 2012) and South American (Chiessi et al. 2009; Kayano and Capistrano 2014). Similarly, the AMO's influence extends to polar SAT and sea ice cover (Chylek et al. 2009; Simpkins et al. 2014; Li et al. 2014).

Recent findings underscore the collective impact of the IPO/PDO and AMO on global climate variability (Joshi and Rai 2015; Li et al. 2016a, b; Si and Ding 2016; Kim et al. 2017; Zhang et al. 2018, 2020; Elsbury et al. 2019; Huang et al. 2019; Kayano et al. 2019, 2020). For instance, Joshi and Rai (2015) examined the combined influence of the AMO and IPO on low-frequency variability of rainfall and extremes over India and its homogeneous monsoon regions, revealing an interconnectedness that resonates throughout East Asian winter and summer monsoon climates. Moreover, the relationship between El Niño-Southern Oscillation (ENSO) and South American rainfall is modulated by the phases of the IPO and AMO (Kayano et al. 2019, 2020). The joint impact of a positive AMO phase and a negative IPO phase can deepen the Amundsen Sea Low (ASL), thereby influencing SAT anomalies around Antarctica (Li et al. 2021). Additionally, Yu and Zhong (2018), along with Yu et al. (2019), attributed over 40% of Arctic sea ice loss over the past four decades to the phase reversal of the PDO and AMO. They further suggested that over half of the opposing trends in Arctic and Antarctic sea ice extents stem from shifts in the phases of the IPO/PDO and AMO (Yu et al. 2017; 2022).

While prior research has explored the joint influence of the IPO/PDO and AMO on Antarctic SAT, they have predominantly focused on the combined influence during the recent four decades when the two indices have been primarily in opposite phases (Yu and Zhong 2018; Yu et al. 2017; 2019; 2022; Li et al. 2021). Fewer studies have delved into the nuanced impacts stemming from the four distinct combinations of the IPO/PDO and AMO phases. In the current study, we undertake an extensive examination of the effects of the four possible phase combinations of IPO and AMO (+IPO+AMO, -IPO-AMO, +IPO-AMO, -IPO+AMO) on Antarctic SAT over the past seven decades using observational and reanalysis datasets and the composite analysis technique. The spatiotemporal variability of the PDO and IPO closely resembles each other (Newman et al. 2016), which is why, in this study, we employ the terminology of IPO and AMO to represent low-latitude SST anomalies on decadal timescales.

Datasets and methods

For the basis of our analysis, we obtained SST data from the U.S. National Oceanic and Atmospheric Administration (NOAA) Extended Reconstructed SST

(ERSST) version 5 dataset. This global SST dataset is reconstructed from in-situ buoy and ship observations, with a temporal resolution of monthly data points and a spatial resolution of 2.0 degrees latitude by 2.0 degrees longitude (Huang et al. 2017). While the ERSSTv5 dataset spans observations dating back to 1854 and continues to the present day, our analysis focuses on the recent seven decades spanning 1948 through 2022. This selection was made in accordance with findings highlighted by Schneider and Fogt (2018) that pointed out that the lack of assimilated observations and notable uncertainties associated with pressure measurements prior to our study period render the dataset's accuracy questionable for our purpose of analysis.

The IPO index is defined as the difference between the SST anomalies averaged over the central equatorial Pacific (10°S–10°N, 170°E–90°W) and the average of the SST anomalies in the Northwest (25°N–45°N, 140°E–145°W) and Southwest (50°S–15°S, 150°E–160°W) Pacific regions (Henley et al. 2015). The AMO index is defined as the area-weighted average of SST anomalies over the North Atlantic Ocean (0°–70°N) (Enfield et al. 2001). The IPO and AMO indices are calculated by the NOAA's Physical Science Laboratory and made available at the following websites: https://psl.noaa.gov/data/timeseries/IPOTPI/tpi.timeseries.ersstv5.data and https://psl.noaa.gov/data/correlation/amon.us.data, respectively. Following the procedure outlined by Hong et al. (2022), both unfiltered indices were detrended and standardized based on their respective standard deviations.

Atmospheric variables were extracted from the European Centre for Medium-Range Weather Forecasts (ECMWF) fifth-generation reanalysis dataset, ERA5, which has a 1/4 degree latitude and longitude horizontal resolution (Hersbach et al., 2020). An additional atmospheric variable, the outgoing longwave radiation (OLR) at the top of the atmosphere, was obtained from NOAA's Interpolated OLR dataset. The Rossby wave source (RWS) and wave activity flux (WAF) were computed following the formulations described in Sardeshmukh and Hoskins (1988) and Takaya and Nakamura (2001), respectively. The primary methodology employed in our study was composite analysis, with statistical significance determined through a two-tailed Student's t-test.

The analysis is based primarily on seasonal anomalies of SST and atmospheric variables, calculated by removing their linear trends and the 1948–2022 climatological means for each of the Antarctic seasons. These seasons are defined as follows: summer (January——March; JFM), autumn (April——June; AMJ), winter (July——September; JAS), and spring (October——December; OND).

Due to constraints in our dataset (Schneider and Fogt 2018), our study was unable to employ longer-term data to create composites of SAT anomalies over the decadal to interdecadal timescales, which are primarily associated with the IPO and AMO. Applying a 20-year filter to our current dataset significantly reduced the sample size for combinations of the IPO and AMO indices in the same phase. To maintain sufficient degrees of freedom in our composite analysis, we opted to use unfiltered IPO and AMO indices. This approach enabled us to examine SAT anomalies across a broader timescale, ranging from interannual to interdecadal variability. Similar methodologies have been employed by Hong et al. (2022) in their examination of tropical interactions between the Pacific and Atlantic Oceans using PDO and AMO indices. Future studies will explore the impacts of IPO and AMO indices on Antarctic SAT if more robust Antarctic SAT data become available. Additionally, pacemaker experiments offer a valuable tool to assess the effects of IPO and AMO on Antarctic SAT.

Results

Anomalous SST patterns corresponding to the IPO and AMO phase combinations

During austral winter, both the IPO and AMO indices exhibit notable interdecadal variability, as depicted in Fig. 1a, b. For instance, the AMO index demonstrates a pattern of positive values spanning from 1948 to 1962 and then again from 1995 to 2022, with a period of negative values in between. In contrast, the interdecadal variability of the IPO index shows predominantly positive values from 1976 to 1997, with a mix of positive and negative values occurring during other periods. The simultaneous correlation coefficient between the IPO and AMO indices registers at −0.18 ($p > 0.05$).

In terms of spatial patterns, SST anomalies during the positive phase of the IPO are characterized by a distinctive horseshoe-shaped positive center, flanked by negative centers in both the central North and South Pacific, as well as the tropical western Pacific Oceans (Fig. 1c). Furthermore, a positive tropical dipole structure is observed in the tropical Indian Ocean, alongside a quadrupole structure extending from the North Atlantic to the South Atlantic. Conversely, during the positive phase of the AMO, a basin-wide warming pattern becomes evident across the North Atlantic Ocean. This warming is accompanied by elevated SSTs in the northwestern and southwestern regions of the Pacific Oceans (Fig. 1d).

To investigate the influence of the IPO and AMO phase interactions on Antarctic SAT, we construct four distinct SST composites based on the positive and negative phases of the two indices, resulting in four combinations: + IPO + AMO, -IPO-AMO, + IPO-AMO,

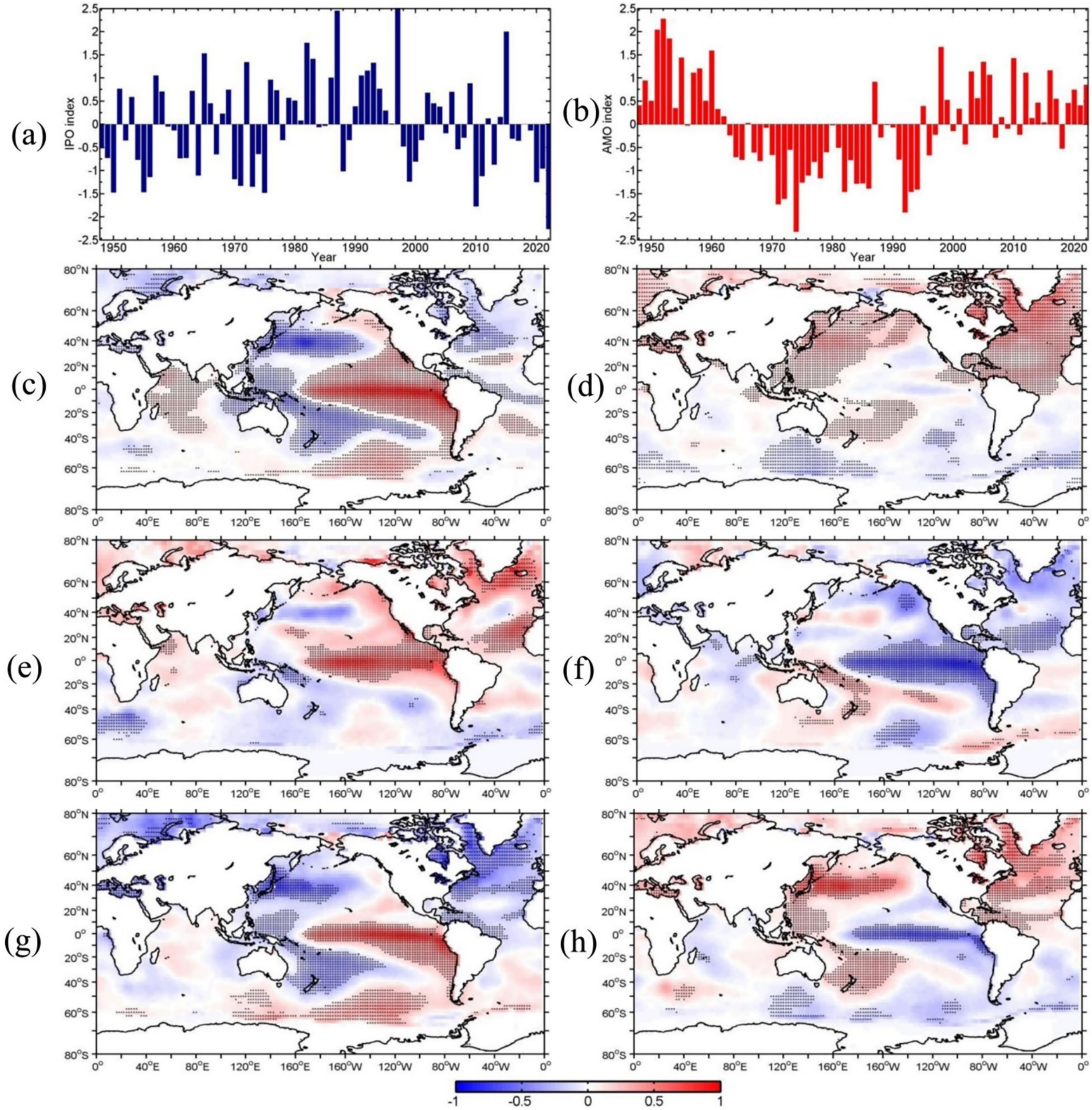

Fig. 1 The detrended and standardized time series of the IPO (**a**) and AMO (**b**) indices in austral winter (JAS) from 1948 to 2022, the spatial patterns of the regressed SST anomalies onto the detrended standardized IPO (**c**) and AMO (**d**) indices (°C), and the composited SST anomalies (°C) for the four IPO and AMO phase combinations: + IPO + AMO (**e**), -IPO-AMO (**f**), + IPO-AMO (**g**), and -IPO + AMO (**h**). Dotted regions indicate the above 95% confidence level

and -IPO + AMO (Table S1). The spatial patterns of SST anomalies corresponding to these combinations are depicted in Figs. 1e-1h. Notably, the SST anomalies corresponding to the two in-phase combinations (+ IPO + AMO and -IPO-AMO) exhibit a mirror-like symmetry (Fig. 1e, f).

However, some differences emerge in the SST spatial patterns when examining the in-phase and out-of-phase combinations of the IPO and AMO indices. For instance, the tropical SST anomalies for + IPO + AMO and -IPO-AMO combinations exhibit nearly symmetrical distributions about the equator (Figs. 1e, f), whereas + IPO-AMO and -IPO + AMO combinations predominantly feature these anomalies in the Southern Hemisphere (Figs. 1g, h). In the case of the in-phase combinations, basin-scale SST anomalies are influenced by disturbances in the central North Atlantic, while for the out-of-phase combinations, these disturbances manifest in the tropical northern Atlantic Ocean.

Overall, the spatial patterns of the IPO and AMO modes for the four combinations (Figs. 1e–h) exhibit some variations compared to the typical patterns (Figs. 1c, d), indicating an interaction between the Pacific and Atlantic basins on interdecadal timescales. Details of specific years corresponding to these four combinations categorized by the phases of the IPO and AMO indices for other seasons can be found in Tables S2-S4, and their spatial representations are illustrated in Figures S1-S3. It is important to note that other seasons exhibit analogous characteristics, both in terms of the temporal variations and spatial patterns.

Anomalous Antarctic SAT patterns corresponding to the IPO and AMO phase combinations

We investigated the influence of the interaction between the IPO and AMO characterized by the four phase combinations on Antarctic SAT for each season, and the results are shown in Fig. 2. Notably, the response of SAT to these four combinations exhibit a distinct seasonal pattern, with the magnitude and extent of SAT anomalies being most prominent during austral winter, followed by austral autumn, and least noticeable in austral summer.

Although the SST anomalies associated with the two in-phase combinations (+IPO + AMO and -IPO-AMO) exhibit a mirror-like symmetry (Figs. 1e, f), the corresponding anomalous SAT patterns are not entirely mirrored. For instance, during austral winter, significant negative SAT anomalies associated with + IPO + AMO occur over the southeastern Pacific Ocean (Fig. 2i). In contrast, SAT anomalies linked to -IPO-AMO exhibit a structure of zonal wave number two with negative values

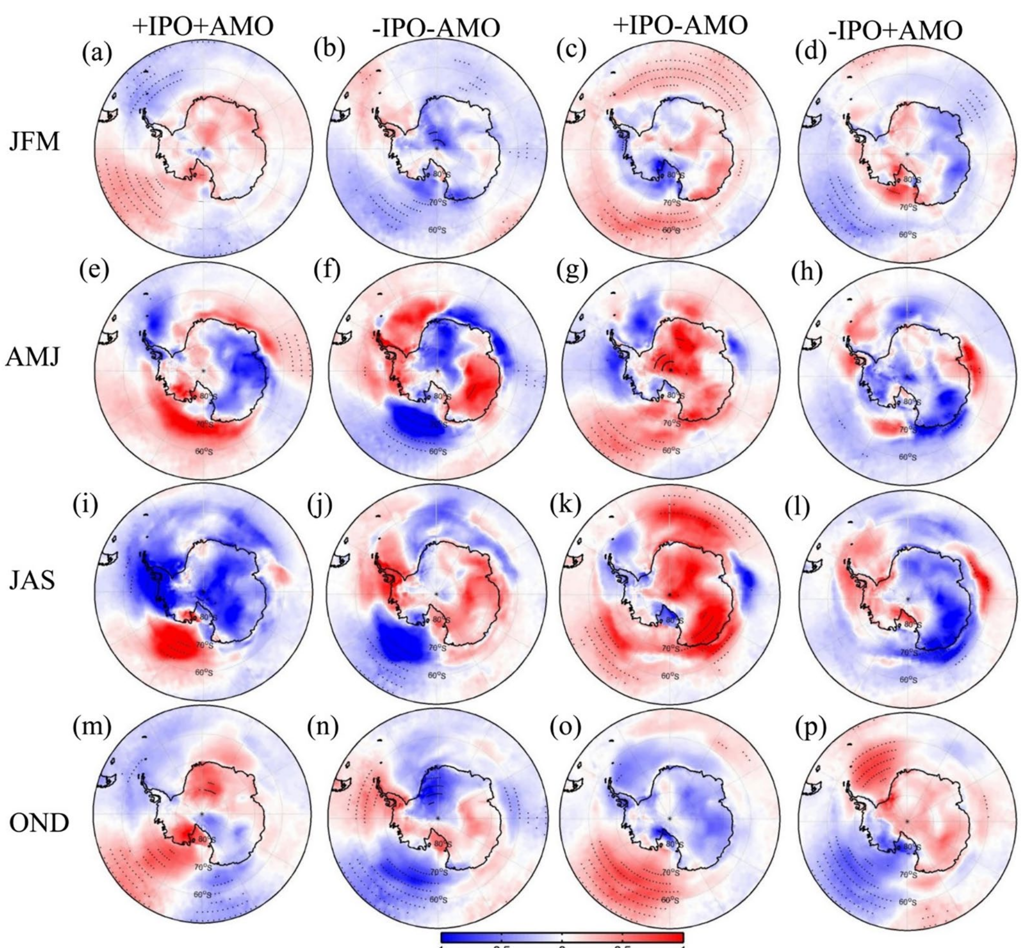

Fig. 2 Anomalous surface air temperature for the four phase combinations of IPO and AMO: + IPO + AMO, (**a**), (**e**), (**i**), (**m**); -IPO-AMO, (**b**), (**f**), (**j**), (**n**); + IPO-AMO, (**c**), (**g**), (**k**), (**o**); and -IPO + AMO, (**d**), (**h**), (**l**), (**p**); in austral summer (JFM), (**a**), (**b**), (**c**), (**d**); autumn (AMJ), (**e**), (**f**), (**g**), (**h**); winter (JAS), (**i**), (**j**), (**k**), (**l**); and spring (OND), (**m**), (**n**), (**o**), (**p**). Dotted regions indicate the above 95% confidence level

also extending over the southern Atlantic and Indian Oceans (Fig. 2j). However, the spatial patterns of SAT anomalies associated with the two out-of-phase combinations (+IPO-AMO and -IPO+AMO) are entirely opposite to each other (Figs. 2k, l). While anomalous SATs in austral autumn and spring for+IPO+AMO and -IPO-AMO both display a zonal wave number two structure, there are slight differences in their location and extent (Figs. 2e, f, m, n).

Additionally, the results show the phase of AMO can modulate the IPO's influence on Antarctic SAT. The extent of positive SAT anomalies in the Southern Pacific Ocean varies depending on the phase of the AMO (Figures S4a, S4c, S4e, S4g, 2). During austral autumn, the negative phase of the AMO diminishes the extent of positive SAT anomalies in the Southern Pacific Ocean induced by the positive phase of the IPO (Figures S4c, 2e, 2 g). Conversely, the opposite occurs for the other seasons (Figures S4a, S4c, S4e, S4g, 2a, 2c, 2i, 2 k, 2 m, 2o). Similarly, the phase of the IPO also affects SAT anomalies related to the AMO (Figures S4b, S4d, S4f, S4h, 2). For instance, there is large difference in the SAT anomalies over the southeastern Pacific Ocean for+IPO+AMO (Fig. 2i), -IPO+AMO (Fig. 2l), and+AMO (Figure S4f). SAT anomalies over the Southern Atlantic Ocean for -IPO-AMO (Figs. 2b–j) during austral summer and winter are nearly opposite to those for+IPO-AMO (Figs. 2c–k).

Mechanisms

Prior research has established that the teleconnection between tropical SST anomalies and Antarctic SAT anomalies is mediated by the Rossby wavetrain initiated by SST anomalies (Li et al. 2021). Given the most significant SAT anomalies occur during austral winter, we focus on elucidating the mechanisms underlying the influence of the four IPO and AMO phase combinations on Antarctic SAT during this season. Detailed insights into the mechanisms during other seasons are provided in the supplementary materials.

During the periods with the+IPO+AMO combination, the positive IPO enhances convective precipitation over the tropical central Pacific Ocean and the central and southeastern Pacific Ocean, while reduces rainfall over the southwestern Pacific Ocean and south of Australia (Figure S5a). The former corresponds to positive RWS and 200-hPa divergent wind patterns, whereas the latter generates the opposite response

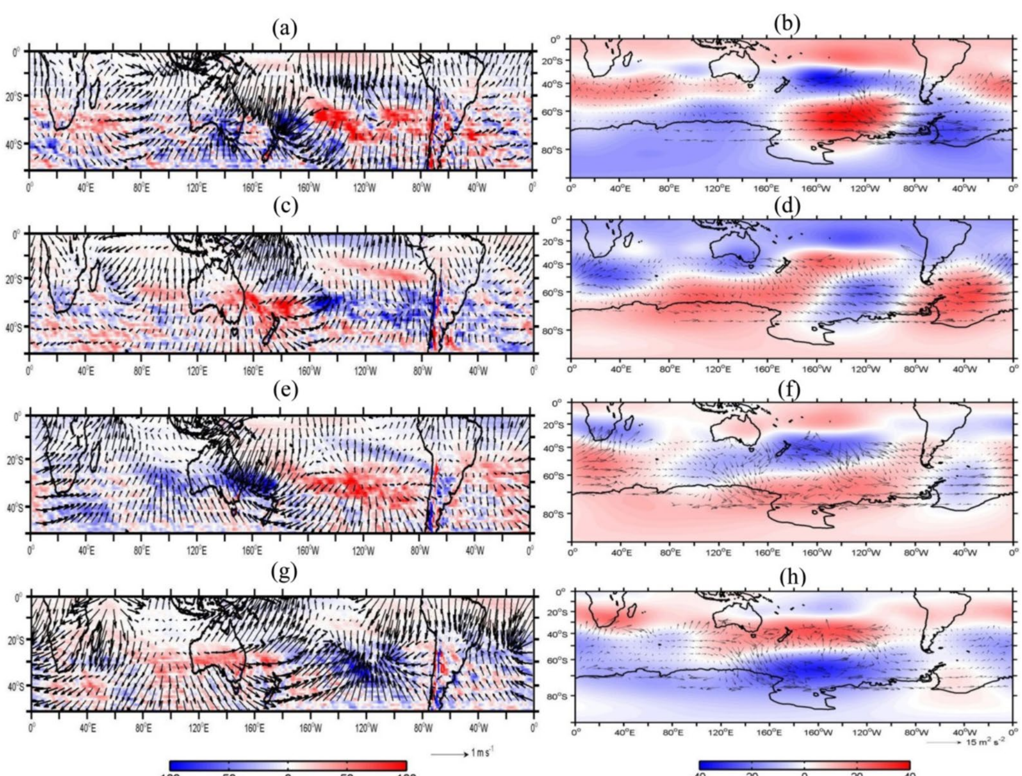

Fig. 3 The composited Rossby wave source (shading) (10^{-10} s^{-2}) and 200-hPa divergent wind (vector), (**a**), (**c**), (**e**), (**g**); wave activity flux (vector) and 200-hPa geopotential height (shading) (gpm), (**b**), (**d**), (**f**), (**h**) in austral winter (JAS) for the four IPO and AMO combinations: + IPO + AMO, (**a**), (**b**); -IPO-AMO, (**c**), (**d**); + IPO-AMO, (**e**), (**f**); and -IPO + AMO, (**g**), (**h**)

(Fig. 3a). These RWS patterns set in motion a Rossby wavetrain that propagates southeastward into the Amundsen, Bellingshausen, and Weddell Seas (Fig. 3b), which results in anomalous 200-hPa geopotential height patterns (Fig. 3b) and mean sea level pressure distributions (Fig. 4a), characterized by a weakened

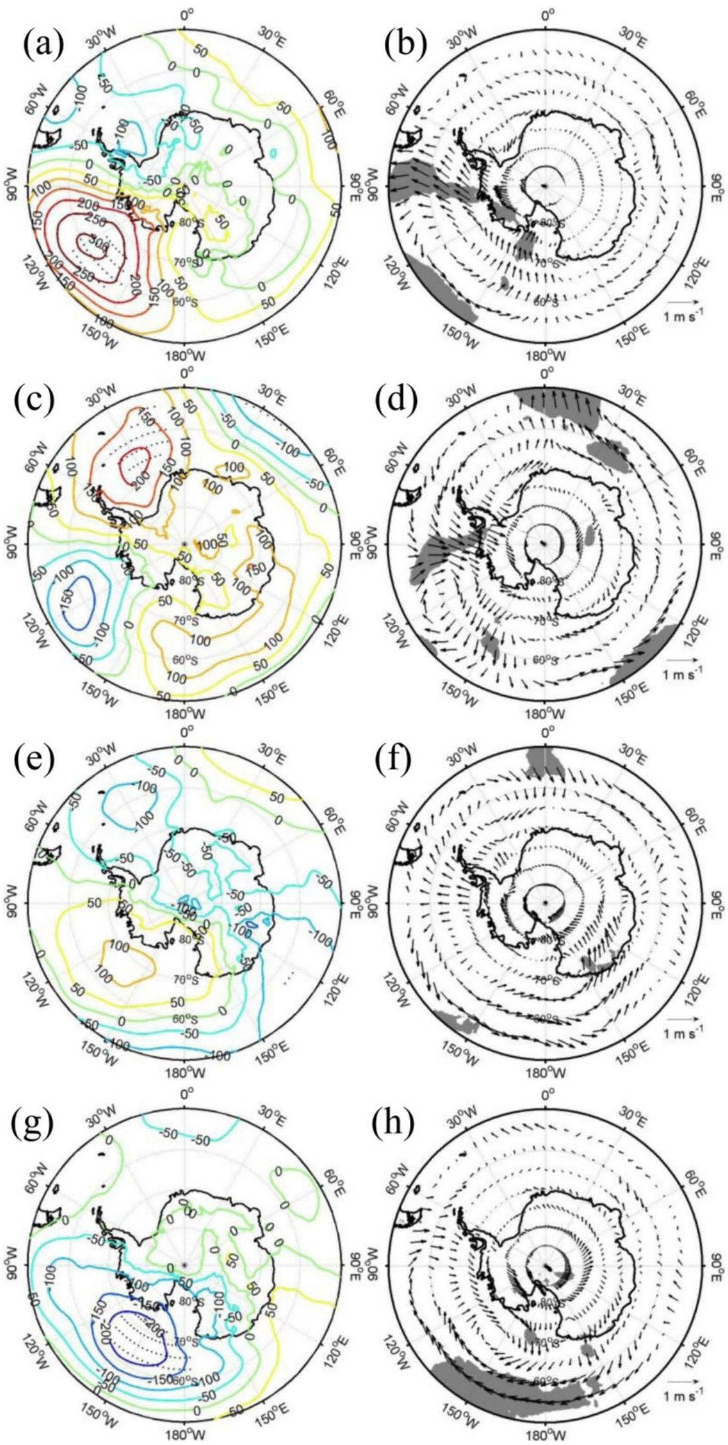

Fig. 4 The composited mean sea level pressure (Pascal), (**a**), (**c**), (**e**), (**g**) and 10 m wind field, (**b**), (**d**), (**f**), (**h**), in austral winter (JAS) for the four IPO and AMO phase combinations: + IPO + AMO, (**a**), (**b**); -IPO-AMO, (**c**), (**d**); + IPO-AMO, (**e**), (**f**); and -IPO + AMO, (**g**), (**h**). Dotted in panels **a**, **c**, **e**, and **g** and shaded regions in panels **b**, **d**, **e**, and **h** indicate the above 95% confidence level

ASL and anomalous low pressure over the Weddell Sea. This weakened ASL generates anomalous northerly winds to the west of its center and anomalous southwesterly winds to the east of its center (Fig. 4b), resulting in positive SAT anomalies over the Ross and western Amundsen Seas, along with negative SAT anomalies over the eastern Amundsen, Bellingshausen, and western Weddell Seas (Fig. 2i). The SAT anomalies over the southern Indian Ocean are also influenced by the associated anomalous surface wind field. Furthermore, the positive SAT anomalies are reinforced by anomalous downward longwave radiation, particularly over East Antarctica (Fig. 5a), with a spatial pattern resembling that of the anomalous SAT in austral winter when there is no shortwave radiation.

During the period with the -IPO-AMO combination, nearly opposite patterns of rainfall anomalies occur over the southern Pacific Ocean (Figure S5b). This generates positive RWS extending from southeastern Australia to the southwestern Pacific and negative RWS over the central to southeastern Pacific Ocean (Fig. 3c). These anomalous RWS patterns excite a wavetrain that propagates southeastward into the Ross, Amundsen, Bellingshausen, and Weddell Seas, along with the southern Indian Oceans (Fig. 3d). The wavetrain results in a strengthened ASL, surrounded by positive mean sea level pressure anomalies (Fig. 4c). The intensified ASL is linked to SAT anomalies that oppose those observed during the + IPO + AMO combination, spanning from the Ross Sea to the western Weddell Sea, as

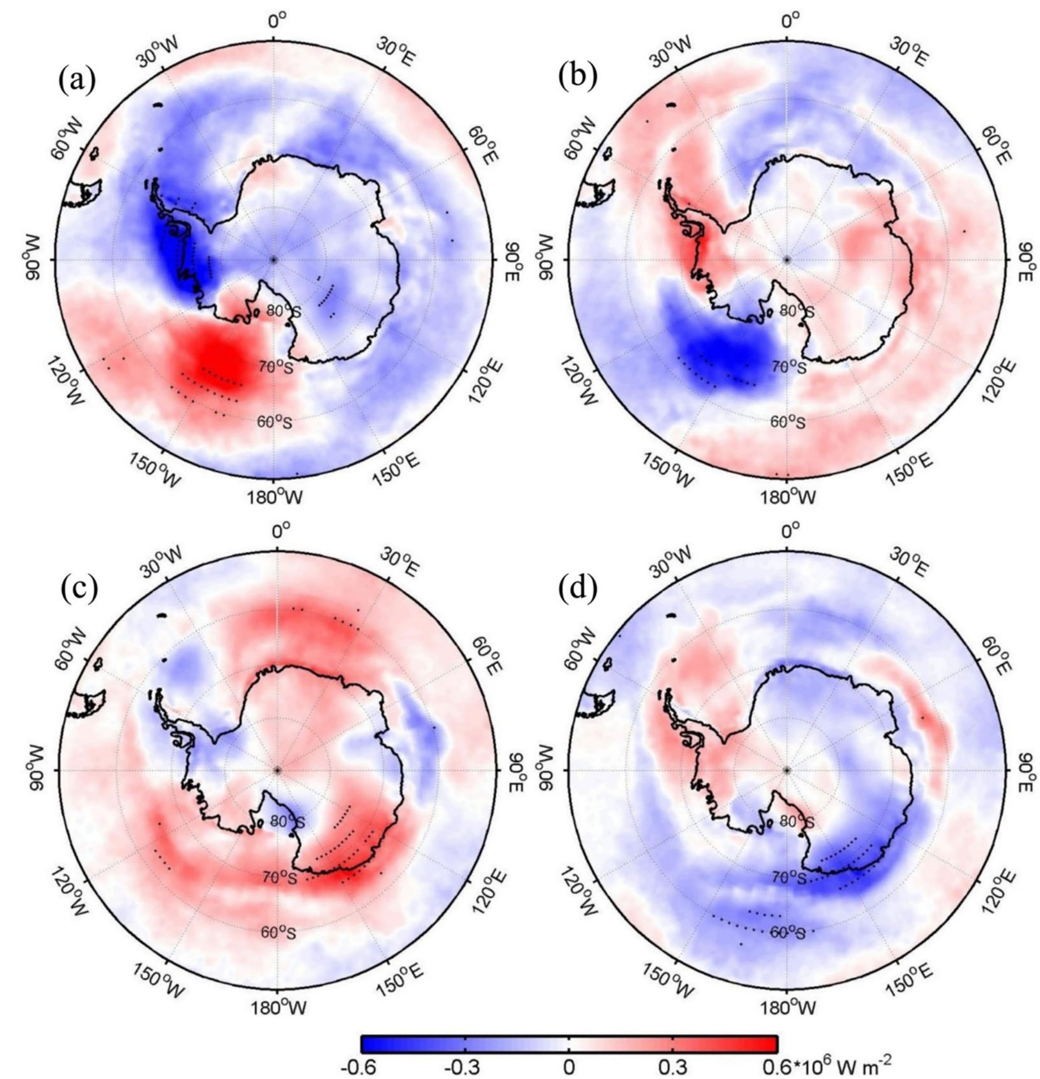

Fig. 5 The composited accumulated downward longwave radiation (10^6 W m^{-2}) in austral winter (JAS) for the four IPO and AMO phase combinations: + IPO + AMO, (**a**); -IPO-AMO, (**b**); + IPO-AMO, (**c**); and -IPO + AMO, (**d**). Dotted regions indicate the above 95% confidence level

indicated by the anomalous surface wind field (Fig. 4d). Anomalous southerly winds, stemming from the positive sea level pressure anomalies over the Weddell Sea, induce negative SAT anomalies over the southern Atlantic Ocean (Fig. 2j). Similarly, SAT anomalies are influenced by anomalous downward longwave radiations (Fig. 5b).

During the period with the + IPO-AMO combination, the spatial patterns of convective activities appear quite similar to those observed during + IPO + AMO (Figure S5c). However, the extent of significant rainfall anomalies over the southern Pacific Ocean and south of Australia during + IPO-AMO is somewhat smaller than that during + IPO + AMO. Conversely, there are more suppressed convective activities over the southwestern Indian Ocean. Consequently, the RWS over the southern Pacific Ocean trigger the development of a distinct wavetrain propagating into the Southern Ocean (Figs. 3e, f). The presence of negative RWS patterns between Australia and New Zealand encourages the formation of the wavetrain. The wavetrain lead to the weakening of the ASL. Although the magnitude of the anomalous ASL is somewhat smaller during + IPO-AMO, its spatial extent is larger than that observed during + IPO + AMO (Fig. 4e). The anomalous northerly winds, associated with this ASL change (Fig. 4f), contribute to the expansion of positive SAT anomalies from the Amundsen Sea to the southeastern Indian Ocean (Fig. 2k). Conversely, the negative SAT anomalies linked to anomalous southerly winds exhibit a smaller spatial extent and magnitude. Two negative anomalous sea level pressure centers, flanking the anomalous ASL, give rise to SAT anomalies over the southern Atlantic and Indian Oceans through the anomalous surface wind field.

Lastly, during the period with the-IPO + AMO combination, a notable pattern emerges with negative RWS over the southern Pacific Ocean and positive RWS over the southern Indian Ocean (Fig. 3g), both associated with rainfall anomalies (Figure S5d). These opposing RWS patterns trigger a distinct wavetrain that propagate southeastwards into the Southern Ocean (Fig. 3h). The wavetrain results in a stronger ASL anomaly, which exhibits a larger spatial extent than that observed during -IPO-AMO (Fig. 4g). The anomalous surface wind field (Fig. 4h), driven by this intensified ASL, induces increased SAT over the Weddell and Bellingshausen Seas and decreased SAT over the Ross Sea and the Southern Indian Ocean. Notably, the negative SAT anomalies over the Southern Indian Ocean correspond to the presence of anomalous northerly winds (Fig. 4h). Additionally, the spatial pattern of downward longwave radiation anomalies (Fig. 5d) closely mirrors that of the anomalous SAT (Fig. 2l).

In summary, during austral winter, each of the four phase combinations of the IPO and AMO indices reveals distinct spatial patterns of SST anomalies. These differences in SST patterns give rise to varying convective activities, subsequently initiating different wavetrains that propagate into the Southern Ocean. These wavetrains, unique to each combination, in turn, induce specific patterns of sea level pressure, surface wind fields, and downward longwave radiation anomalies. The culmination of these processes ultimately results in diverse patterns of Antarctic SAT anomalies. It is worth noting that analogous mechanisms are in play during the other three seasons, as illustrated in Figures S6 to S10.

Conclusions and discussions

In this study, we analyzed global SST (ERSSTv5) and atmospheric (ERA5) datasets during the period from 1948 to 2022 to understand the interactions between the Pacific and Atlantic basins, contingent on the four possible phase combinations of the IPO and AMO modes, and their influence on the Antarctic SAT anomalies and their seasonal variations.

The Pacific-Atlantic interaction results in distinct spatial patterns of SST anomalies for the four phase combinations of the IPO and AMO indices. These patterns deviate somewhat from the typical patterns observed for the individual indices, reflecting the mutual influence and feedback between the two basins. Our findings demonstrate that the impact of one index on Antarctic SAT is contingent upon the phase of the other. Notably, the Antarctic SAT anomalies related to these combinations exhibit a clear seasonal character, with the most substantial anomalies occurring during austral winter, followed by austral autumn, and the smallest occurring in austral summer.

The varying SST anomalies associated with these combinations trigger distinct convective rainfall patterns, in turn initiating different wavetrains that propagate into the Southern Ocean. These wavetrains give rise to varying sea level pressure and surface wind field patterns, which, through the mechanisms of horizontal thermal advection and downward longwave radiation, lead to diverse Antarctic SAT anomalies.

Previous studies have examined the impacts of the four phase combinations of the IPO and AMO indices but with a focus on tropical Pacific Climate, Indian monsoon rainfall, and East Asian climate. Antarctic climate studies, however, have primarily centered on the out-of-phase combinations of the two indices, which have been predominant over the recent four decades. To the best of our knowledge, our study is the first to comprehensively examine the effects of all four combinations of the IPO and AMO phases on Antarctic SAT.

Our study highlights the atmospheric pathways through which the tropical and subtropical signals of IPO and AMO and their phase combinations can influence Antarctic SAT. However, we cannot rule out the role of the oceanic pathways in the connection between IPO/AMO and Antarctic SAT. Previous studies have examined these oceanic pathways. The Atlantic meridional overturning circulation (AMOC) related to the AMO can impact the opposite variability of SAT over the North Atlantic Ocean and the Southern Ocean/Antarctic continent (Johnsen et al. 1972; Blunier and Brook 2001; Stocker and Johnsen 2003; Kim et al. 2020). The mode shift of the AMOC also contributes to warming over the Southern Ocean (Oka et al. 2021). Additionally, ENSO can modulate the SST anomalies over the Southern Ocean through heat anomalies related to Ekman currents (Ciasto and England 2011).

While our analysis is based on the ERA5 reanalysis dataset for the past seven decades, we acknowledge that the limited data length may introduce some uncertainty. Future research will benefit from employing longer-term, reliable datasets and conducting numerical experiments to augment our understanding and reduce uncertainties stemming from limited sample size. The insights gained from this study regarding the connection between Antarctic SAT and SST anomalies in the tropical Pacific and Atlantic Oceans hold potential for enhancing our ability to predict shifts and fluctuations in Antarctic SAT. It is important to emphasize that even slight alterations in Antarctic SAT can exert profound repercussions on the stability of ice sheets and, consequently, on the global issue of rising sea levels.

Supplementary Information

The online version contains supplementary material available at https://doi.org/10.1186/s40562-024-00352-8.

Supplementary Material 1.

Acknowledgements
This research would not have been feasible without access to the invaluable ERA5 dataset generously provided by the European Centre for Medium——Range Weather Forecasts (ECMWF) and the ERSST dataset made accessible by NOAA's Physical Science Laboratory. Their data resources played an indispensable role in our study. This study is financially supported by the National Key R&D Program of China (2022YFE0106300), the National Science Foundation of China (41941009), and the fundamental research funds for the Norges Forskningsråd. (No. 328886).

Author contributions
L.Y. designed the story line, analyzed the data, and wrote the draft. S.Z. contributed in writing and revising of the paper. C.S. analyzed wave activity flux and wave source. B.S. offered the revised suggestion.

Funding
The National Key R & amp; D Program of China, 2022YFE0106300, Lejiang Yu

Availability of data and materials
The analysis utilized publically available climate datasets that can be downloaded from websites. In particularly, the monthly SST data from the U.S. NOAA Extended Reconstructed Sea Surface Temperature (ERSST) can be downloaded from https://www1.ncdc.noaa.gov/pub/data/cmb/ersst/v5/netcdf/); the ERA5 reanalysis data can be downloaded from https://doi.org/https://doi.org/10.24381/cds.6860a573; the monthly outgoing longwave raidation data are available at https://psl.noaa.gov/data/gridded/data.uninterp_OLR.html.

Declarations

Competing interests
The authors declare no competing interests.

Author details
[1]MNR Key Laboratory for Polar Science, Polar Research Institute of China, Shanghai, China. [2]Department of Geography, Environment and Spatial Sciences, Michigan State University, East Lansing, MI, USA. [3]Key Laboratory of Marine Hazards Forecasting, Ministry of Natural Resources, National Marine Environmental Forecasting Center, Beijing, China.

Received: 1 April 2024 Accepted: 3 August 2024
Published online: 22 August 2024

References
An X, Wu B, Zhou T, Liu B (2021) Atlantic multidecadal oscillation drives interdecadal Pacific variability via tropical atmospheric bridge. J Climate 34:5543–5553
Andreoli RV, Kayano MT (2005) ENSO-related rainfall anomalies in South America and associated circulation features during warm and cold Pacific decadal oscillation regimes. Int J Climatol 25:2017–2030
Blunier T, Brook EJ (2001) Timing of millennial-scale climate change in Antarctica and Greenland during the last glacial period. Science 291:109–112
Cai W, Wu L, Lengaigne M, Li T, McGregor S, Kug J-S, Yu J-Y et al (2019) Pan-tropical climate interactions. Science. https://doi.org/10.1126/science.aav4236
Chan JC, Zhou W (2005) PDO, ENSO and the early summer monsoon rainfall over south China. Geophys Res Lett 32:L08810
Chen W, Feng J, Wu R (2013) Roles of ENSO and PDO in the link of the East Asian winter monsoon to the following summer monsoon. J Climate 26:622–635
Chiessi CM, Mulitza S, Pätzold J, Wefer G, Marengo JA (2009) Possible impact of the atlantic multidecadal oscillation on the South American summer monsoon. Geophys Res Lett 36:L21707
Chylek P, Folland CK, Lesins G, Dubey MK, Wang M (2009) Arctic air temperature change amplification and the Atlantic Multidecadal Oscillation. Geophys Res Lett 36:L14801
Ciasto LM, England MH (2011) Observed ENSO teleconnections to Southern Ocean SST anomalies diagnosed from a surface mixed layer heat budget. Geophys Res Lett 38:L09701
D'Orgeville M, Peltier WR (2007) On the Pacific decadal oscillation and the Atlantic multidecadal oscillation: Might they be related? Geophys Res Lett 34:L23705
Dong B, Dai A (2015) The influence of the interdecadal Pacific oscillation on temperature and precipitation over the globe. Climate Dyn 45:2667–2681
Elsbury D, Peings Y, Saint-Martin D, Douville H, Magnusdottir G (2019) The atmospheric response to positive IPV, positive AMV, and their combination in boreal winter. J Climate 32:4193–4213
Enfield DB, Mestas-Nunez AM, Trimble PJ (2001) The Atlantic multidecadal oscillation and it's relation to rainfall and river flows in the continental U.S. Geophys Res Lett 28:2077–2080
Henley BJ, Gergis J, Karoly DJ, Power SB, Kennedy J, Folland CK (2015) A tripole index for the interdecadal Pacific oscillation. Clim Dyn 45:3077–3090
Hersbach H, Bell B, Berrisford P, Hirahara S, Horányi A, Muñoz-Sabater J, et al (2020). The ERA5 global reanalysis. Q. J. Roy. Meteor. Soc., 146, 1999–2049.

Hessl AE, McKenzie D, Schellhaas R (2004) Drought and Pacific decadal oscillation linked to the fire occurrence in the inland Pacific Northwest. Ecol Appl 14:425–442
Hong J-S, Yeh S-W, Yang Y-M (2022) Interbasin interactions between the Pacific and Atlantic oceans depending on the phase of Pacific decadal oscillation and Atlantic multidecadal oscillation. J Climate 35:2883–2894
Huang B, Thorne PW, Banzon VF, Zhang HM (2017) Extended reconstructed Sea surface Temperature version 5 (ERSSTv5), Upgrades, validations, and Intercomparisons. J Climate 30:8179–8205
Huang D, Dai A, Yang B, Yan P, Zhu J, Yang Y (2019) Contributions of different combinations of the IPO and AMO to recent changes in winter East Asian jets. J Climate 32:3384–3397
Johnsen S, Dansgaard W, Clausen H, Langway C (1972) Oxygen isotope profiles through the Antarctic and Greenland ice sheets. Nature 235:429–434
Joshi MK, Rai A (2015) Combined interplay of the Atlantic multidecadal oscillation and the interdecadal Pacific oscillation on rainfall and its extremes over Indian subcontinent. Climate Dyn 44:3339–4335
Kayano MT, Capistrano VB (2014) How the Atlantic Multidecadal Oscillation (AMO) modifies the ENSO influence on the South American rainfall. Int J Climatol 27:531–540
Kayano MT, Andreoli RV, de Souza RAF (2019) El Niño-Southern Oscillation related teleconnections over South America under distinct Atlantic Multidecadal Oscillation and Pacific Interdecadal Oscillation backgrounds: La Niña. Int J Climatol 39:1359–1372
Kayano MT, Andreoli RV, de Souza RAF (2020) Pacific and Atlantic multidecadal variability relations to the El Nino events and their effects on the South American rainfall. Int J Climatol 40:2183–2200
Kayanom MT, Andreoli RV (2007) Relations of South American summer rainfall interannual variations with the Pacific decadal oscillation. Int J Climatol 27:531–540
Kim JW, An SI, Jun SY, Park H-J, Yeh S-W (2017) ENSO and East Asian winter monsoon relationship modulation associated with the anomalous northwest Pacific anticyclone. Climate Dyn 49:1157–1179
Kim D, Lee S-K, Lopez H, Goes M (2020) Pacific mean-state control of Atlantic Multidecadal Oscillation-El Niño relationship. J Climate 33:4273–4291
Knight JR, Folland CK, Scaife AA (2006) Climate impacts of the Atlantic multidecadal oscillation. Geophys Res Lett 33:L17706
Kosaka Y, Xie S-P (2013) Recent global-warming hiatus tied to equatorial Pacific surface cooling. Nature 501:403–407
Krishnamurthy L, Krishnamurthy V (2014) Influence of PDO on South Asian summer monsoon and monsoon-ENSO relation. Climate Dyn 42:2397–2410
Krishnan R, Sugi M (2003) Pacfiic decadal oscillation and variability of the Indian summer monsoon rainfall. Climate Dyn 21:233–242
Levine AF, MePhaden MJ, Frierson DM (2017) The impact of the AMO on multidecadal ENSO variability. Geophys Res Lett 44:3877–3886
Li X, Holland DM, Gerber EP, Yoo C (2014) Impacts of the north and tropical Atlantic Ocean on the Antarctic Peninsula and sea ice. Nature 505:538–542
Li X, Xie S-P, Gille T, Yoo C (2016a) Atlantic induced pan-tropical climate change over the past three decades. Nat Climate Change 6:275–279
Li AK, Pack H, Yu J-Y (2016b) The changing influences of the AMO and PDO on the decadal variation of the Santa Ana winds. Environ Res Lett 11:064019
Li X, Cai W, Meehl GA, Chen D, Yuan X, Raphael M et al (2021) Tropical teleconnection impacts on Antarctic climate changes. Nat Rev Earth Environ 2:680–698
Mantua NJ, Hare SR (2002) The Pacific decadal oscillation. J Oceanogr 58:35–44
Mantua NJ, Hare SR, Zhang Y, Wallace JM, Francis RC (1997) A Pacific interdecadal climate oscillation with impacts on salmon production. Bull Amer Meteor Soc 78:1069–1080
Martin ER, Thorncroft CD (2014) The impact of the AMO on the West African monsoon cycle. Quart J Roy Meteor Soc 140:31–46
McGregor S, Timmermann A, Stuecker F, England H, Merrifield M, Jin F-F, Chikamoto Y (2014) Recent walker circulation strengthening and Pacific cooling amplified by Atlantic warming. Nat Climate Change 4:888–892
Meehl GA, Hu A, Arblaster JM, Fasullo J, Trenberth KE (2013) Externally forced and internally generated decadal climate variability associated with the interdecadal Pacific oscillation. J Climate 26:7298–7310
Meehl GA, Arblaster JM, Bitz CM, Chung CT, Teng H (2016) Antarctic sea-ice expansion between 2000 and 2014 driven by tropical Pacific decadal climate variability. Nat Geosci 9:590–595
Meehl GA, Chung CT, Y., Arblaster, J. M., Holland, M. M., & Bitz, C. M. (2018) Tropical decadal variability and the rate of Arctic sea ice decrease. Geophys Res Lett 45:11326–11333
Meehl GA, Arblaster JM, Vhung CTY, Holland MM, DuVivier A, Thompson L (2019) Sustained ocean changes contributed to sudden Antarctic sea ice retreat in late 2016. Nat Commun 10:1–9
Meehl GA, Hu A, Castruccio F, England MH, Bates SC, Danabasoglu G (2021) Atlantic and Pacific tropics connected by mutually interactive decadal-timescale processes. Nat Geosci 14:36–42
Newman M, Alexander MA, Ault TR, Cobb KM, Deser C, Di Lorenzo E (2016) The Pacific decadal oscillation, revisited. J Climate 29:4399–4427
Oka A, Abe-Ouchi A, Sherriff-Tadano S, Yokoyama Y, Kawamura K, Hasumi H (2021) Glacial mode shift of the Atlantic meridional overturning circulation by warming over the Southern Ocean. Commun Earth Environ 2:169
Peings Y, Magnusdottir G (2014) Forcing of the wintertime atmospheric circulation by the multidecadal fluctuations of the North Atlantic Ocean. Environ Res Lett 9:034018
Peings Y, Magnusdottir G (2016) Wintertime atmospheric response to Atlantic multidecadal variability: dependence on stratospheric representation and ocean–atmosphere coupling. Climate Dyn 47:1029–1047
Ruprich-Robert Y, Msadek R, Castruccio F, Yeager S, Delworth T, Danabasoglu G (2017) Assessing the climate impacts of the observed Atlantic multidecadal variability using the GFDL CM2.1 and NCAR CESM1 global coupled models. J Climate 30:2785–2810
Sardeshmukh PD, Hoskins BJ (1988) The generation of global rotational flow by steady idealized tropical divergence. J Atmos Sci 45:1228–1251
Schneider DP, Fogt RL (2018) Artifacts in century-length atmospheric and coupled reanalyses over Antarctica due to historical data availability. Geophys Res Lett 45:964–973
Si D, Ding Y (2016) Oceanic forcings of the interdecadal variability in East Asian summer rainfall. J Climate 29:7633–7649
Simpkins GR, Mcgregor S, Taschetto AS, Ciasto LM, England MH (2014) Tropical connections to climatic change in the extratropical Southern Hemisphere: the role of Atlantic SST trends. J Climate 27:4923–4936
Sutton RT, Hodson DLR (2005) Atlantic ocean forcing of North American and European summer climate. Science 309:115–118
Takaya K, Nakamura H (2001) A formulation of a phase in dependent wave-activity flux for stationary and migratory quasi geostrophic eddies on a zonally varying basic flow. J Atmos Sci 58:608–627
Thomas FS, Sigfùs JJ (2003) A minimum thermodynamic model for the bipolar seesaw. Paleoceanography 8:1–9
Turner J, Lu H, White I, King JC, Phillips T, Hosking JS (2016) Absence of 21st century warming on Antarctic Peninsula consistent with natural variability. Nature 535:411–415
Turner J, Marshall GJ, Clem K, Colwell S, Phillips T, Lu H (2020) Antarctic temperature variability and change from station data. Int J Climatol 40:2986–3007
Vimont DJ, Kossin JP (2007) The Atlantic meridional mode and hurricane activity. Geophys Res Lett 34:L07709
Wang L, Chen W, Huang R (2008) Interdecadal modulation of PDO on the impact of ENSO on the East Asian winter monsoon. Geophys Res Lett 35:L20702
Wang C, Dong S, Evan AT, Foltz GR, Lee S-K (2012) Multidecadal covariability of North Atlantic sea surface temperature, African dust, Sahel rainfall, and Atlantic hurricanes. J Climate 25:5404–5415
Wu S, Liu Z, Zhang R, Delworth TL (2011) On the observed relationship between the Pacific Decadal Oscillation and the Atlantic multi-decadal Oscillation. J Oceanogr 67:27–35
Yu L, Zhong S (2018) Changes in sea-surface temperature and atmospheric circulation patterns associated with reductions in Arctic sea ice cover in recent decades. Atmospheric Chem Phys 18:14149–14159
Yu L, Zhong S, Winkler JA, Zhou M, Lenschow DH, Li B (2017) Possible connections of the opposite trends in Arctic and Antarctic sea-ice cover. Sci Rep 7:45804
Yu L, Zhong S, Zhou M, Lenschow DH, Sun B (2019) Revisiting the linkages between the variability of atmospheric circulations and Arctic melt-season sea ice cover at multiple time scales. J Climate 32:1461–1482
Yu L, Zhong S, Sun B (2022) Synchronous variation patterns of monthly sea ice anomalies at the Arctic and Antarctic. J Climate 35:2823–2847

Zhang Z, Sun X, Yang X-Q (2018) Understanding the interdecadal variability of East Asian summer monsoon precipitation: Joint influence of three oceanic signals. J Climate 31:5485–5506

Zhang G, Zeng G, Li C, Yang X (2020) Impact of PDO and AMO on interdecadal variability in extreme high temperatures in North China over the most recent 40-year period. Climate Dyn 54:3003–3020

Publisher's Note